FINAL

CONF-820662--6

HIGH-TEMPERATURE OXIDATION OF ZIRCALOY IN HYDROGEN-STEAM MIXTURES*

CONF-820662--6

DE83 014687

H. M. Chung
Materials Science Division
Argonne National Laboratory
Argonne, Illinois 60439

and

G. R. Thomas
Nuclear Safety Analysis Center
Electric Power Research Institute
Palo Alto, California 94303

9500767

September 1982

DISCLAIMER

This report was prepared as an account of work sponsored by an agency of the United States Government. Neither the United States Government nor any agency thereof, nor any of their employees, makes any warranty, express or implied, or assumes any legal liability or responsibility for the accuracy, completeness, or usefulness of any information, apparatus, product, or process disclosed, or represents that its use would not infringe privately owned rights. Reference herein to any specific commercial product, process, or service by trade name, trademark, manufacturer, or otherwise does not necessarily constitute or imply its endorsement, recommendation, or favoring by the United States Government or any agency thereof. The views and opinions of authors expressed herein do not necessarily state or reflect those of the United States Government or any agency thereof.

MASTER

Paper presented at the Sixth International Conference on Zirconium in the Nuclear Industry, Vancouver, Canada, June 28-July 1, 1982.

*Work supported by the Nuclear Safety Analysis Center, Electric Power Research Institute, Palo Alto, CA.

DISTRIBUTION OF THIS DOCUMENT IS UNLIMITED

EHB

HIGH-TEMPERATURE OXIDATION OF ZIRCALOY IN HYDROGEN-STEAM MIXTURES*

H. M. Chung
Materials Science Division
Argonne National Laboratory
Argonne, Illinois 60439

and

G. R. Thomas
Nuclear Safety Analysis Center
Electric Power Research Institute
Palo Alto, California 94303

ABSTRACT

Oxidation rates of Zircaloy-4 cladding tubes have been measured in hydrogen-steam mixtures at 1200-1700°C. For a given isothermal oxidation temperature, the oxide layer thicknesses have been measured as a function of time, steam supply rate, and hydrogen overpressure. The oxidation rates in the mixtures were compared with similar data obtained in pure steam and helium-steam environments under otherwise identical conditions. The rates in pure steam and helium-steam mixtures were equivalent and comparable to the parabolic rates obtained under steam-saturated conditions and reported in the literature. However, when the helium was replaced with hydrogen of equivalent partial pressure, a significantly smaller oxidation rate was observed. For high steam-supply rates, the oxidation kinetics in a hydrogen-steam mixture were parabolic, but the rate was smaller than for pure steam or helium-steam mixtures. Under otherwise identical conditions, the ratio of the parabolic rate for hydrogen-steam to that for pure steam decreased with increasing temperature and decreasing steam-supply rate. The smaller parabolic rates in

*Work supported by the Nuclear Safety Analysis Center, Electric Power Research Institute, Palo Alto, CA.

the hydrogen-steam mixtures indicate that, under the test conditions, a considerable amount of hydrogen was dissolved in Zircaloy during oxidation, and as a consequence, oxygen transport in both the oxide and alpha phases was slower than in the corresponding phases produced in pure steam or helium-steam mixtures. The findings are discussed in relation to some reported high-temperature transport characteristics of oxygen ions in the oxide formed in hydrogen-steam mixtures. For smaller steam-supply rates (sufficiently small but still larger than the "steam starvation" limit), significantly smaller linear oxidation rates were observed in the hydrogen-steam mixture, which indicate that the oxidation rate was limited either by the gaseous transport of the steam molecules or as a result of chemical reaction between the chemisorbed oxygen on the ZrO_2 surface and the gaseous hydrogen molecules. This phenomenon of "hydrogen blanketing" is discussed in relation to fuel-rod heatup in a degraded-core-accident situation.

KEY WORDS: Zircaloy-4, oxidation, hydrogen-steam mixture, hydrogen-blanketing, oxygen ion transport, anion vacancy, hydrogen dissolution, degraded-core accident.

HIGH-TEMPERATURE OXIDATION OF ZIRCALOY IN HYDROGEN-STEAM MIXTURES*

H. M. Chung
Materials Science Division
Argonne National Laboratory
Argonne, Illinois 60439

and

G. R. Thomas
Nuclear Safety Analysis Center
Electric Power Research Institute
Palo Alto, California 94303

INTRODUCTION

An understanding of the kinetics and thermochemistry of reactions involving Zircaloy fuel cladding, hydrogen-steam mixtures, and UO_2 fuel pellets is crucial for proper analysis of the core heatup and damage occurring during a degraded-core accident in a water-cooled reactor. During such an event, exemplified by the TMI-2 accident, a large amount of hydrogen can be generated as a result of Zircaloy oxidation and the upper core region is expected to be exposed to a mixture of hydrogen and depleted steam rather than to an unlimited flux of pure steam. To provide a better understanding of the high-temperature oxidation behavior of Zircaloy in hydrogen-steam mixtures, oxidation experiments under simulated degraded-core-accident conditions have been performed.

The effects of hydrogen gas on the high-temperature oxidation rates of zirconium or Zircaloy have been reported by several investigators. Westerman measured weight gains of Zircaloy-2 specimens as a function of time during oxidation at 750°C in 1.33 kPa steam and in a mixture of 1.33 kPa steam and 6.67 kPa hydrogen.[1] Weight gain, corrected for hydrogen uptake, in the

*Work supported by the Nuclear Safety Analysis Center, Electric Power Research Institute, Palo Alto, CA.

hydrogen-steam mixture was approximately half of that measured in pure steam. This smaller weight gain in the mixture was attributed to a limitation of the oxidation rate by the gaseous diffusion of steam molecules. However, no further results have been reported that would have clarified the mechanism of the rate limitation, e.g., a comparison of oxidation kinetics measured in hydrogen-steam and helium-steam mixtures under otherwise identical conditions. Reaction rates of Zircaloy-4 ring specimens have been reported as a function of hydrogen-steam ratio by Homma et al.[2] Increased weight gain and accelerated oxidation due to breakaway-type porous oxide formation have been reported for volume ratios ranging from 0.3 to 0.5 at 1000-1100°C. For volume ratios $\geq$0.6, weight gain was significantly smaller in the hydrogen-steam mixture than in pure steam for the same temperature range. These results have limited applicability for analysis of severe-core-damage accidents because (1) a significant fraction of hydrogen in the coolant channel is likely to be produced only at high temperatures, e.g., $\geq$1400°C, (2) information on the growth rates of the oxide and alpha layers is required for correlation with the heat generation rate and fuel rod damage, and (3) the smaller weight gain for volume ratios $\geq$0.6 may actually have been due to the extremely small steam supply rate rather than any effect of mixed hydrogen. The breakaway oxidation described by Homma et al. was later reported to be limited to ~1140°C based on oxidation studies of deformed and ruptured Zircaloy-4 fuel cladding tubes under simulated accident conditions.[3] This means that the oxidation rate in hydrogen-steam mixtures can be equal to or less than the rate in pure steam at temperatures of $\geq$1200°C; i.e., for conditions of interest during primary fuel-rod cladding oxidation and hydrogen generation in a degraded-core-accident situation. Cathcart et al.[4] reported no significant effect of 5 mol % hydrogen, mixed with steam, on the oxidation kinetics of Zircaloy-4 at

1100-1300°C. This finding for a low hydrogen fraction appears to be consistent with the information reported by Homma et al.[2]

In view of the limited information on and inconclusive evidence for the effect of hydrogen on the Zircaloy oxidation rates, we have conducted a series of oxidation experiments in pure steam, hydrogen-steam, and helium-steam mixtures under a wider range of conditions, especially under conditions that are believed to be more important for understanding the fuel-rod behavior in a degraded-core-accident situation, i.e., higher cladding temperatures (>1200°C) and higher hydrogen fractions (>0.5).

EXPERIMENTAL PROCEDURES

Material and Specimen Geometry

The material used in this investigation was Zircaloy-4 cladding tubes (outside diameter 10.9 mm, wall thickness 0.635 mm). The test specimens were cut from tube 7FD12, which has been analyzed and described in detail elsewhere.[3] The tubing was ~80% cold-worked and stress-relieved at 500°C for 4 h. The material had the following chemical composition (in weight percent): 1.50 tin, 0.20 iron, 0.12 chromium, 0.12 oxygen, 0.0057 nitrogen, 0.0035 carbon, and 0.0014 hydrogen. The 90-mm-long specimen was ultrasonically cleaned in alcohol, and positioned vertically in the reaction chamber as schematically illustrated in Fig. 1. The bottom end of the specimen was tightly sealed to prevent the steam or the hydrogen-steam mixture from entering the specimen inner space. However, the top end was left partially open to simulate the fuel cladding rupture that is expected to occur in a degraded-core-accident situation. Consequently, the specimen inner surface was exposed to a hydrogen-rich environment containing a limited amount of steam; this environment was similar to those reported for the cladding

inner surface in several earlier studies of simulated fuel rod rupture and oxidation studies.[3,5,6]

Test Procedure

The reaction chamber illustrated in Fig. 1 can be routinely evacuated to ~1 Pa and filled with a mixture of the desired gas components through a gas-handling system. Superheated steam was generated from distilled water by a metering pump and heater and was supplied to the reaction chamber through heated valves and tubes. Actual steam supply rates from the mixture outlet were calibrated by capturing the steam outflow through a condenser circuit. The calibrated steam supply rate in the gas mixture was equal to the metered water pumping rate. Research-grade hydrogen was supplied through a calibrated flowmeter from a separate tank.

A limited number of data were obtained with steam supply rates >4 g/min, under conditions in which the uniformly mixed gases flowed past the specimen surface and were pumped out. Most of the data were obtained with the reaction chamber isolated from the pump. The chamber was evacuated to a pressure of $\leq_1$ Pa, isolated, supplied with steam, and filled with hydrogen or helium at room temperature to a total pressure of 33.4 kPa. Steam was supplied through four holes (diameter ~1.5 mm) arranged at 90° intervals around the middle level of the specimen, ~17 mm away from the specimen outer surface. The attachment point of the center thermocouple and the focal point of the infrared pyrometer were also located at this level. The steam molecules reached the specimen surface via natural convection in the stagnant hydrogen or helium.

The specimen was heated by ac power self-resistance. Specimen temperature was controlled by a feedback circuit of the power supply driven by the amplified signal from an infrared pyrometer. Power input to the specimen was adjusted automatically 20 times per second to maintain a preprogrammed surface

adjusted automatically 20 times per second to maintain a preprogrammed surface brightness temperature. The infrared pyrometer was calibrated against Pt-Pt 10% Rh and W-W 26% Re thermocouples in the following way: Both types of thermocouples were spot-welded directly to the unoxidized outer surface of the specimen tube in the middle axial level on which the pyrometer was focused. Then the specimen was heated to the melting point (i.e., ~1860°C) at a rate of 5-10°C/s (driven by a preprogrammed data track) in a desired gas mixture environment. Three temperature signals, simultaneously produced from the same axial level of the specimen by the pyrometer, Pt-Pt 10% Rh, and W-W 26% Re thermocouples, were displayed on a strip chart recorder. As the oxide layer built up on the specimen surface during the transient heating, the emissivity of the oxide surface reached a stabilized near-constant value and good linear correlations between the pyrometer and thermocouple signals were obtained. Although low-melting eutectics are known to form at ~1185, 1660, and 1600°C for Zr-Pt, Zr-W, and Zr-Re systems, respectively, signals obtained during the transient oxidation at $\lesssim$1500 and $\lesssim$1670°C from the Pt-Pt 10% Rh and W-W 26% Re thermocouples, respectively, were not erratic. To convert the thermocouple outputs to true temperatures, it was necessary to take account of thermal shunting effects. The effects were calibrated separately by comparing two slightly different signal outputs that were measured from a preoxidized specimen in vacuo and in a stagnant gas mixture, respectively, under conditions of identical surface brightness. The resultant pyrometer calibrations obtained with two different types of thermocouples were nearly identical over the range (1200-1500°C) in which the signal outputs overlapped. Extrapolated pyrometer calibration curves were used to determine temperatures >1670°C.

Some typical temperature-time profiles from our experiments are shown in Fig. 2. In both cases depicted in Fig. 2, the specimen temperature was

controlled primarily by the infrared pyrometer. However, in some hydrogen-steam mixtures, e.g., a steam supply rate of 0.13 g/min with a hydrogen overpressure of ~33 kPa at 1452°C (see Fig. 3), the oxidation rate and, hence, the oxide layer buildup were still small at the end of the transient oxidation period. As a result, emissivity was not stable and it was not possible to maintain constant specimen temperature by means of the pyrometer-controlling mode. In such cases, the temperature was controlled by a thermocouple for a short period of isothermal oxidation (e.g., ~30 s at 1452°C) until a sufficiently thick oxide layer was built up. A switch was then made to the pyrometer control mode. Because of eutectic formation, temperature control by a thermocouple signal was possible only for short periods of high-temperature oxidation.

Typically, it took 7-10 min to establish and calibrate a constant steam supply. During this period, some steam condensed in the bell jar, and the pressure in the chamber increased to 1.3-4 kPa for steam supply rates of 0.13-2 g/min. When the specimen was heated to 1200-1700°C for oxidation without hydrogen or helium overpressure, the bell jar pressure increased to 2.1-8.1 kPa, with the exact pressure depending on steam supply rate, isothermal oxidation temperature, and oxidation time. The pressure increase was primarily due to the vaporization of condensed steam as the specimen and bell jar surfaces were heated. For oxidation tests in gas mixtures, hydrogen or helium was added to the bell jar along with the steam to bring the room temperature total pressure to 33.4 kPa. Then the specimen was heated to the desired isothermal oxidation temperature as shown in Fig. 2. At the end of an oxidation run, the system pressure increased to 38.5-44 kPa. The total pressure was higher for a larger steam supply rate. However, for an identical

steam supply rate, the total pressure was also slightly dependent on the test temperature and duration.

After each oxidation test, the specimen was sectioned at the axial level containing the pyrometer focal spot and thermocouple welds. The cross section was then mounted, polished, etched, and photographed with a microscope to determine the oxide-, alpha-, and beta-phase layer thicknesses. Typically, 3-4 oxide layer thicknesses were measured at 100X magnification along the circumference of the cross section. For specimens oxidized at >1400°C, it was necessary to normalize the measured oxide layer thickness with respect to the original wall thickness. For example, specimens tested at 1705°C were usually somewhat softened and bent. Therefore, occasionally the plane of the mounted cross section was not perpendicular to the tube axis. In such a case, the observed oxide layer thickness was corrected by the equation

$$X = \frac{W_o}{\frac{X'}{R} + X_\alpha + X_\beta} X', \qquad (1)$$

where X = corrected oxide layer thickness,

W_o = original wall thickness, i.e., 0.635 mm,

R = Pilling-Bedworth ratio, i.e., 1.56,

X', X_α, X_β = observed oxide-, alpha-, and beta-phase layer thickness, respectively.

For some specimens, small brittle chips of oxidized cladding were obtained from near the pyrometer focal spot and analyzed to determine oxygen and hydrogen contents by the inert gas fusion technique. The analysis provided oxygen and hydrogen contents averaged across the whole wall thickness.

RESULTS AND DISCUSSION

Among the various oxidation parameters (e.g., weight gain, amount of hydrogen generated, oxide thickness, oxide plus alpha layer thickness), the square of the oxide layer thickness, plotted as a function of time, is most convenient for determination of the reaction kinetics. Such plots are shown in Figs. 3-6, which summarize data obtained for various gas mixtures and steam supply rates for isothermal oxidation temperatures of 1452, 1216, 1580, and 1705°C, respectively.

Figures 3-6 show significant retardation of oxidation rates by the hydrogen overpressure in the temperature range studied. The retardation effect is more significant for a smaller steam supply rate under otherwise identical conditions. For an identical steam supply rate, it appears that the retardation effect is more pronounced for a higher oxidation temperature, e.g., compare the results of Figs. 3 and 5 obtained at 1452 and 1705°C, respectively.

For all the steam supply rates, the oxidation kinetics in pure steam were invariably parabolic and the rate constants were indeed a function of specimen temperature only. The oxide layer growth rate constants were determined from the slopes for pure steam in Figs. 3-6 and plotted as a function of inverse temperature in Fig. 7. For comparison, similar rate constants reported by Cathcart and Pawel[4] for $\lesssim$1500°C and by Urbanic and Heidrick[7] for up to ~1800°C are also plotted in Fig. 7. A good agreement is evident from the comparison for $\gtrsim$1300°C, the range of primary importance for a degraded-core-accident analysis. The investigation of Urbanic and Heidrick is unique in that it covers temperatures <1800°C and shows a discontinuity of the Arrhenius plot at ~1580°C. They explained that the higher growth rates at >1580°C were because of higher oxygen transport rates in cubic oxide (stable in the higher

temperature range) compared to those in tetragonal oxide. The results of Fig. 7 confirm this finding.

The fact that all the data obtained in pure steam environments can be described by the parabolic rate constants of Fig. 7 show that, for the present experimental conditions in which the steam supply rate was varied as a test parameter, there was no "steam starvation." Steam starvation usually refers to a condition in which the absolute amount of steam available per unit area of specimen surface is not sufficient to sustain the parabolic oxidation rates obtained under steam-saturated conditions. Under the present test conditions, the absolute amount of steam incident on the specimen surface in a pure steam environment, should be larger than the values indicated by the steam supply rates, since the steam that condensed in the bell jar during the 7-10 min of the flow establishment and calibration period was later vaporized when the specimen was heated to that temperature.

Initial oxidation kinetics were not parabolic in hydrogen-steam mixtures with small steam supply rates, e.g., 0.13 g/min at 1216°C (Fig. 4), 0.13 g/min at 1452°C (Fig. 3), and $\lesssim$0.30 g/min at 1705°C (Fig. 6). The nonparabolic oxidation data could be fit to linear kinetics as shown in Figs. 8(A) and (B), which are linear plots of oxide layer thickness vs time for 1216 and 1452°C, respectively. The linear oxidation rates observed for the hydrogen-steam mixtures were in all cases smaller than the parabolic rates obtained in pure steam for a given temperature. This observation strongly indicates that the rate-controlling steps for the linear oxidations of Fig. 8 were either (a) gaseous transport of steam molecules to the oxide surface in the gas mixtures, or (b) surface reaction processes of dissociation of chemisorbed steam molecules (on the oxide surface) and possible recombination of the dissociated oxygen with hydrogen. The latter process, i.e., chemical reduction of

chemisorbed and dissociated oxygen by gaseous hydrogen, has been reported by Smith.[8] Oxidation under conditions similar to those of Fig. 8(A) but in helium-steam mixtures is normally parabolic, as shown in Fig. 4. Since it can be safely assumed that the diffusivities of steam molecules in helium-steam and hydrogen-steam mixtures are nearly equivalent, we can further deduce that the linear oxidation of Fig. 8(A) is controlled by surface processes. With a steam supply rate of 0.5 g/min, the oxidation rate in hydrogen-steam mixtures is no longer limited by the surface reaction steps at the increased temperatures of 1452°C (Fig. 3) and 1705°C (Fig. 6). However, with a steam supply rate of ~0.13 g/min, the early-stage oxidation at 1452°C in the hydrogen-steam mixture showed linear kinetics [Fig. 8(B)]. In this case, oxidation in the helium-steam mixture was also linear, which indicates that the oxidation rate in either helium or hydrogen at 1452°C is limited to some extent by the gaseous diffusion of steam molecules. The oxidation rate in hydrogen-steam is further retarded by the surface reaction steps that follow the gaseous diffusion process. Although similar data were not obtained for helium-steam at 1705°C for steam supply rates of 0.25 and 0.13 g/min, initial oxidation in these environments would also be expected to show linear kinetics.

As the oxide layer thickness increases, the available diffusion flux of oxygen in ZrO_2 at the position of the oxide/alpha-phase boundary is decreased. Thus, eventually the solid-phase diffusion of oxygen determines the overall oxidation kinetics. The corresponding parabolic rate constants are smaller in the hydrogen-steam mixture than in pure steam or in helium-steam. This shows that the hydrogen is dissolved in the Zircaloy cladding to a considerable extent and that the oxygen diffusion is slowed down because of the dissolved hydrogen. Rate limitation by this solid-phase process appears to be more pronounced for the higher temperature under otherwise identical

conditions. This point is illustrated by Fig. 9, in which the ratio of the parabolic oxide layer growth rate constant for hydrogen-steam mixtures to that for unlimited pure steam is plotted as a function of Zircaloy-4 temperature for several steam supply rates.

A general expression for the oxidation rate expected in a hydrogen-steam mixture during a degraded-core-accident situation includes the thermal-hydraulic parameters of the coolant as well as material parameters of the Zircaloy cladding. The oxide layer growth rate can be expressed in general by the equation

$$\frac{dX}{dt} = f\left(T,\ P^S_{H_2},\ P^S_{H_2O},\ X\right), \tag{2}$$

where X = oxide layer thickness,

t = time,

T = cladding temperature,

$P^S_{H_2O}$, $P^S_{H_2}$ = steam and hydrogen partial pressures in the coolant-cladding boundary layer, respectively.

Under a condition of saturated steam, Eq. (2) is simply given by

$$\frac{dX_o}{dt} = \frac{\delta_o(T)}{2X_o} \tag{3}$$

or

$$X_o^2 = X_o^{o2} + \delta_o(T)t, \tag{4}$$

where X_o and δ_o denote oxide layer thickness and growth rate constant, respectively, obtained under conditions of saturated steam, e.g., the results of Fig. 7. Similar equations can be derived for parabolic oxidation in hydrogen-steam mixtures, e.g.,

$$X_P^2 = X_P^{o\,2} + \delta_P\left(T,\ P^S_{H_2},\ P^S_{H_2O}\right)t \ , \qquad (5)$$

where X_P and δ_P denote the oxide layer thickness and the growth rate constant, respectively, in a hydrogen-steam mixture. Therefore, in general, the ratio (F) of δ_P to δ_o is expected to be a function of T, $P^S_{H_2}$, and $P^S_{H_2O}$, i.e.,

$$F\left(T,\ P^S_{H_2},\ P^S_{H_2O}\right) = \frac{\delta_P}{\delta_o} \ . \qquad (6)$$

This F-function should be somewhat different from those of Fig. 9 since the results of Fig. 9 were obtained for a constant steam supply rate which is merely a test parameter rather than a fundamental kinetic parameter, e.g., $P^S_{H_2}$ or $P^S_{H_2O}$. Quantification of $P^S_{H_2}$ or $P^S_{H_2O}$ appears to be a complex problem, since the hydrogen concentration gradient near the oxide surface would be nonuriform because of the flow condition as well as the hydrogen counterflow produced from the oxidation process itself.

It has been generally believed that oxidation of Zr and its alloys takes place via transport of oxygen rather than Zr ions in the oxide phase.[9] Zirconium dioxide is oxygen-deficient (i.e., contains oxygen ion vacancies) when nonstoichiometric. The oxide phase has been believed to be predominantly an intrinsic n-type semiconductor with oxygen transport occurring via anion vacancy diffusion. However, several electrical conductivity studies[10-12] in the 1200-1750°C range provide some evidence for extrinsic p-type conduction of the oxide phase for oxygen pressures $>10^{-5}$ atmosphere. In this pressure range, the conductivity increases slightly for increasing oxygen partial pressure, in contrast to a reverse relationship for oxygen partial pressures of $<10^{-6}$ atmosphere (which indicates n-type conductivity for the lower

pressure range). For the high-pressure range in which p-type conductivity of ZrO_2 is indicated, oxidation rate is expected to decrease somewhat as oxygen partial pressure decreases. Kofstad[9] explained the p-type conductivity on the basis of impurity cations of valence lower than Zr that may have dissolved in the oxide substitutionally. The oxide phase contains oxygen vacancies at a concentration that is determined by the concentration of dissolved cations. According to this model, if hydrogen is dissolved in the oxide to a considerable extent during oxidation in a hydrogen-steam mixture, one would expect a modification of defect concentrations and p-type conductivity in the oxide. Hydrogen ions (i.e., H^+ with a lower valence than Zr ion) dissolved in the oxide either as interstitials or as substitutional cations, would produce an increase in the oxygen vacancy concentration primarily in the oxide layer near the gas phase. Therefore, the oxygen vacancy concentration gradient across the oxide phase would be decreased. As a result, the oxygen transport, and hence the oxidation rate, would be decreased. The oxidation rate would be smaller for a lower oxygen partial pressure, i.e., a lower steam supply rate or a higher hydrogen overpressure in the hydrogen-steam mixtures in our tests.

Our observations on the parabolic growth rates of oxides in hydrogen-steam mixtures, presented in Figs. 3-6 and 9, agree with the above model of oxygen transport in ZrO_2. To determine hydrogen concentrations dissolved in the oxidized material, several specimens were analyzed by the inert-gas fusion technique. Specimens oxidized either in pure steam or in helium-steam mixtures showed hydrogen contents of 100-350 wt ppm. Specimens oxidized in hydrogen-steam mixtures contained higher hydrogen concentrations of 600-2000 wt ppm. The higher concentrations are similar to the values reported from fuel-rod burst and severe-oxidation tests under simulated accident conditions.[3] However, it was not possible to determine the amount of dissolved

hydrogen in the thin oxide at the gas/oxide boundary. We have noticed an unusual pinkish oxide color, similar to that of clay, for all the specimens tested at 1705°C and in a mixture of hydrogen and steam with steam supply rates $\lesssim$0.3 g/min (Fig. 6). For specimens with comparable oxide-layer thickness but oxidized in pure steam or helium-steam mixtures, the oxide color was invariably dark gray. In steam environments, the oxide color gradually changes from light brown to dark brown, violet, dark blue, black, dark gray, gray, and finally to white as the oxide layer thickness increases. Aronson[13] has observed a pinkish oxide color for ZrO_2 powders equilibrated with hydrogen-steam mixtures at 900-1100°C. When similar powders were equilibrated in hydrogen-steam mixtures diluted with helium or argon, the oxide color was the normal gray. By measuring the weight gain in the equilibrated powders during subsequent oxidation in oxygen at 750°C (until stoichiometric oxides with a white color were produced), Aronson determined the nonstoichiometry of the powders equilibrated in different gas mixtures. As pointed out by McClaine and Coppel[12] and by Kofstad,[9] an increase in nonstoichiometry with decreasing temperature at a constant partial pressure of oxygen, as indicated by Aronson's results, is extremely unlikely based on thermodynamic considerations. Thus, McClaine and Coppel[12] have suggested that the nonstoichiometry measurements may have been influenced by large amounts of hydrogen dissolved in Aronson's powder oxide specimens. Our observation of an unusual oxide color appears to agree with this interpretation, i.e., a significant amount of hydrogen dissolved in the oxide phase.

McClaine and Coppel,[12] in their investigation of the electrical conductivity of tetragonal ZrO_2 at 1100-1550°C, have reported increased electronic conductivity (hence, decreased ionic conductivity) in hydrogen-steam mixtures as compared to similar measurements in $CO-CO_2$ mixtures. This was attributed

to the presence of dissolved hydrogen, in the form of a proton with an associated electron, in the matrix ZrO_2 in hydrogen-steam mixtures. If oxygen transport is the primary component of the ionic conductivity, as suggested by McClaine and Coppel, the decreased ionic conductivity observed in the hydrogen-steam mixtures corresponds to slower oxygen transport in the oxide phase. The smaller oxide layer growth rates in hydrogen-steam mixtures observed in the present study (Figs. 3-6 and 9) appear to agree with this model of oxygen transport behavior.

For later stages in a severe-fuel-damage accident in which a fuel-rod cladding is expected to be exposed to a hydrogen-rich coolant atmosphere at very high temperatures (>1700°C), slow oxidation rates similar to those of the lower curves of Fig. 6 would be of particular importance. Since the conditions at a higher temperature would be conducive to a more pronounced hydrogen-blanketing at the coolant-cladding boundary and to a higher content of hydrogen dissolved in the oxide, one would expect a more pronounced oxidation-rate limitation under such conditions.

CONCLUSIONS

1. Oxidation rates for Zircaloy-4 tubes at 1216-1705°C are slower in hydrogen-steam mixtures than in pure steam or helium-steam environments.
2. Oxidation in hydrogen-steam mixtures is parabolic or linear depending on the Zircaloy temperature, pressures of steam and hydrogen at the gas/oxide boundary, and oxide layer thickness. The linear oxidation rates are smaller than the parabolic rates and indicate that the overall oxidation rate is controlled by gaseous diffusion of hydrogen and by surface reaction between the gaseous hydrogen in the boundary layer and chemisorbed oxygen species on the oxide surface.

3. The parabolic oxidation rate in a hydrogen-steam mixture, which is smaller than the corresponding rate in steam, decreases with decreasing partial pressure of oxygen at the gas/oxide interface or increasing hydrogen-to-steam ratio. At temperatures $\geq$1500°C, the retardation of the parabolic oxidation rate relative to pure steam for a given gas flow and hydrogen-steam composition is more pronounced at higher temperatures.
4. The parabolic oxidation behavior in a hydrogen-steam mixture can be explained on the basis of an oxygen transport model of ZrO_{2-x} in which a considerable amount of hydrogen is dissolved in the oxide phase, and as a result, the oxygen vacancy concentration in the oxide near the gas/oxide boundary is increased, thereby reducing the vacancy concentration gradient and oxygen ion transport rate across the oxide layer.

ACKNOWLEDGMENTS

The authors gratefully acknowledge the experimental contributions of L. Burkel, W. K. Soppet, and R. A. Conner. This work was sponsored by the Nuclear Safety Analysis Center, operated by the Electric Power Research Institute, Palo Alto, CA.

REFERENCES

1. R. E. Westerman, "High Temperature Oxidation of Zirconium and Zircaloy-2 in Oxygen and Water Vapor," HW-73511, Hanford Laboratories, Hanford, Washington, April 1962, pp. 21-23.
2. K. Homma, T. Furuta, and S. Kawasaki, "Behavior of Zircaloy Cladding Tube in a Mixed Gas of Hydrogen and Steam," JAERI-7131, Japan Atomic Energy Research Institute, Tokai, Japan, December 1977.

3. H. M. Chung and T. F. Kassner, "Embrittlement Criteria for Zircaloy Fuel Cladding Applicable to Accident Situations in Light-Water Reactors: Summary Report," ANL-79-48, Argonne National Laboratory, Argonne, Illinois, January 1980.

4. J. V. Cathcart, R. E. Pawel, R. A. McKee, R. E. Druschel, G. J. Yurek, J. J. Campbell, and S. H. Jury, "Zirconium Metal-Water Oxidation Kinetics IV. Reaction Rate Studies," ORNL/NUREG-17, Oak Ridge National Laboratory, Oak Ridge, Tennessee, August 1977.

5. H. Uetsuka, T. Furuta, and S. Kawasaki, Journal of Nuclear Science and Technology Vol. 18, 1981, p. 705.

6. T. Furuta, H. Uetsuka, and S. Kawasaki, Journal of Nuclear Science and Technology Vol. 18, 1981, p. 802.

7. V. R. Urbanic and T. R. Heidrick, Journal of Nuclear Materials Vol. 75, 1978, p. 251-261.

8. T. Smith, Electrochemical Technology Vol. 4, 1966, p. 108.

9. P. Kofstad, Nonstoichiometry, Diffusion, and Electrical Conductivity in Binary Metal Oxides, Wiley-Interscience, New York, 1972, pp. 152-165.

10. A. Guillet and A.-M. Anthony, Revue des Hautes Temperatures et Refractaires Vol. 1, 1964, p. 324.

11. R. W. Vest and N. M. Tallan, Journal of the American Ceramic Society Vol. 48, 1965, p. 472.

12. L. A. McClaine and C. P. Coppel, Journal of the Electrochemical Society Vol. 113, 1966, p. 80.

13. S. Aronson, Journal of the Electrochemical Society Vol. 108, 1961, p. 312.

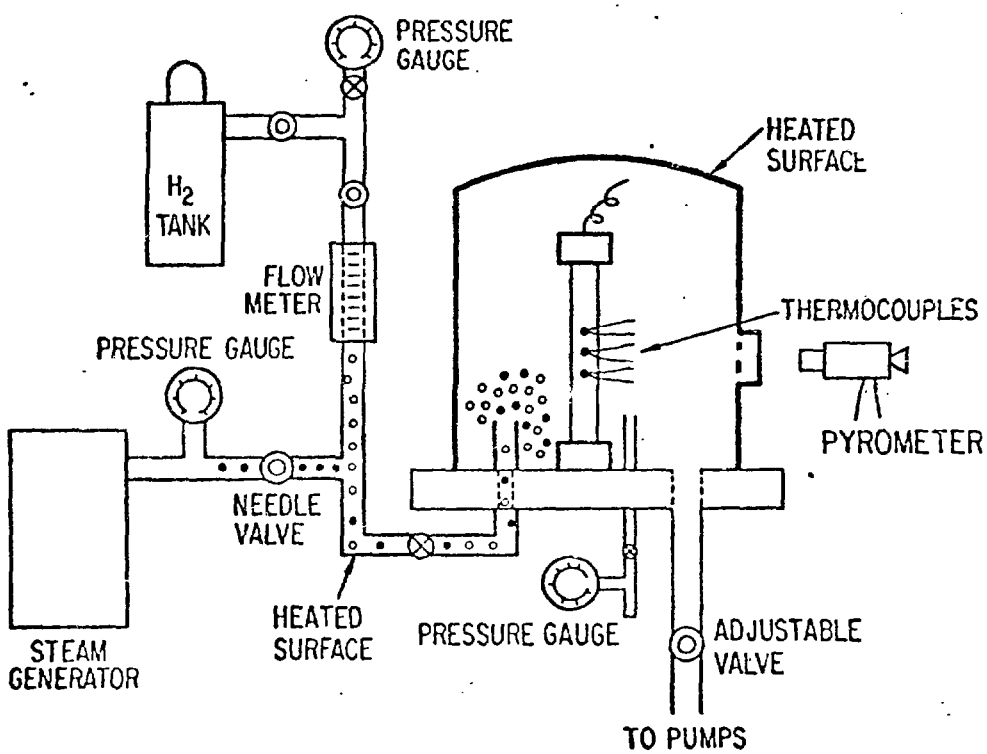

Fig. 1. Apparatus for Zircaloy Oxidation in Hydrogen-Steam Mixtures. The test specimen, with welded thermocouples, is placed in the center of the bell jar facing a pyrometer through a quartz window.

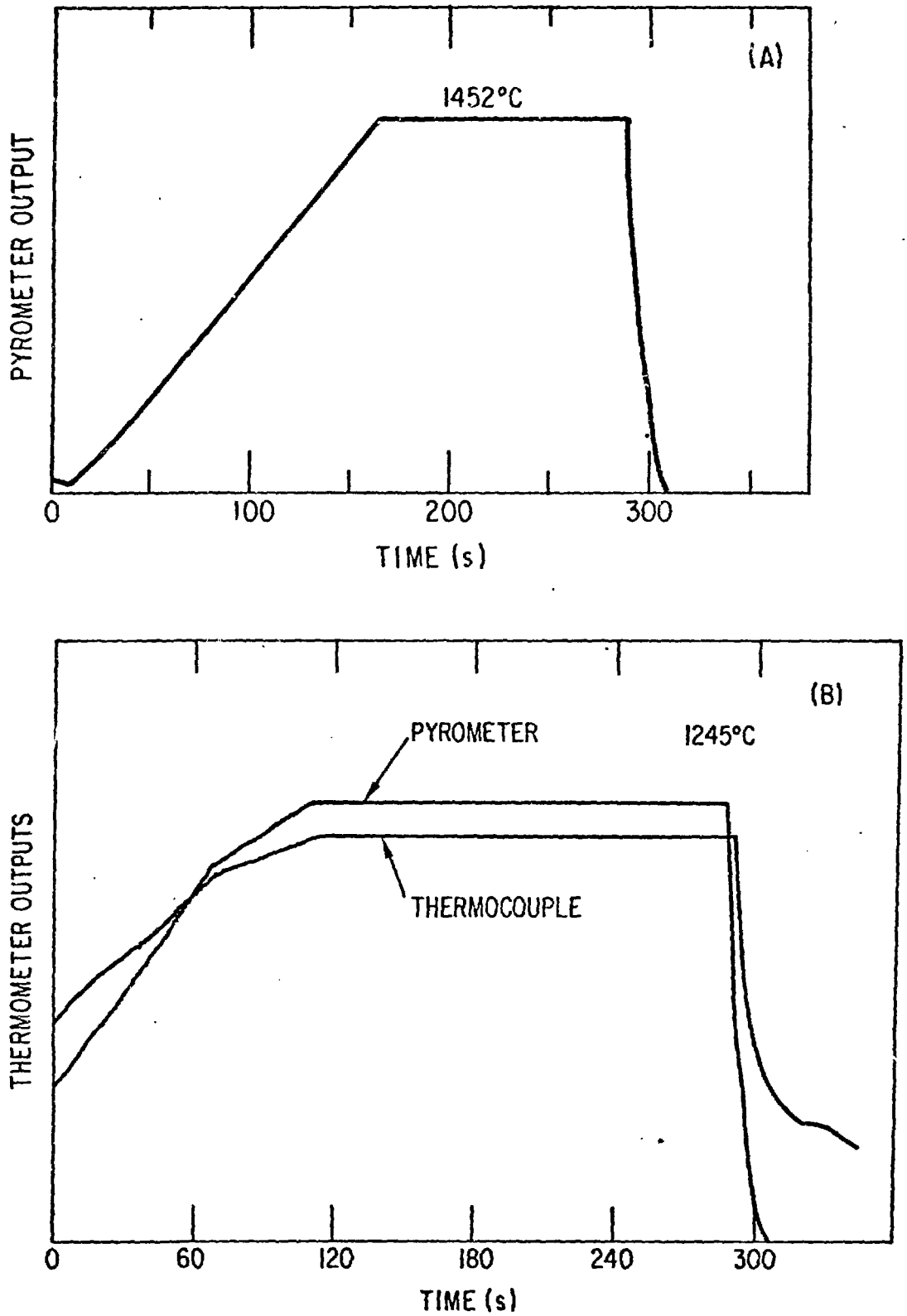

Fig. 2. Typical Temperature-Time Profiles for Zircaloy Oxidation in Hydrogen-Steam Mixtures. (A) A pyrometer record corresponding to an isothermal oxidation temperature of 1452°C, (B) pyrometer and Pt-Pt 10% Rh thermocouple records corresponding to an isothermal oxidation temperature of 1245°C.

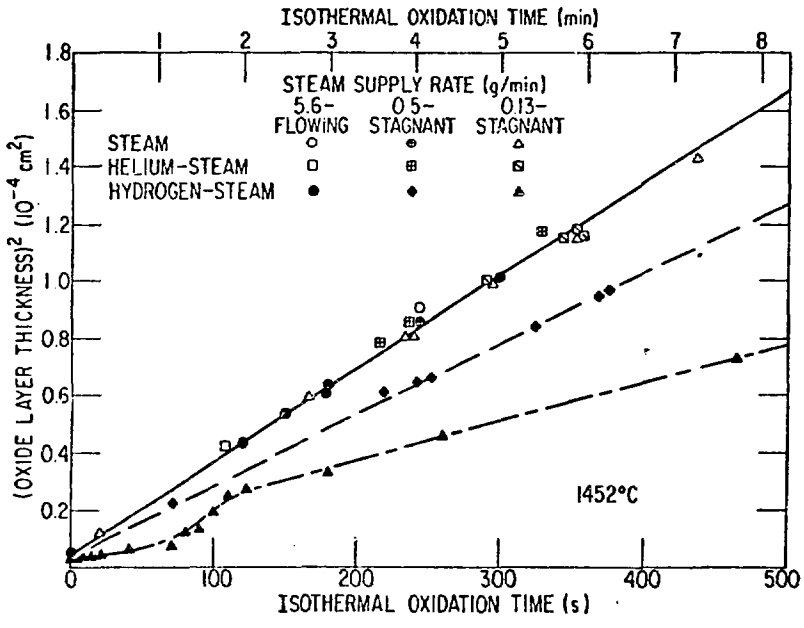

Fig. 3. Square of Oxide Layer Thickness vs Isothermal Oxidation Time Obtained from Zircaloy-4 Oxidation Tests at 1452°C in Pure Steam and Helium-Steam and Hydrogen-Steam Mixtures under Various Steam Flow Conditions. Helium and hydrogen overpressures were essentially identical, i.e., ~33 kPa at 20°C. Total pressures during tests were 38-44 kPa.

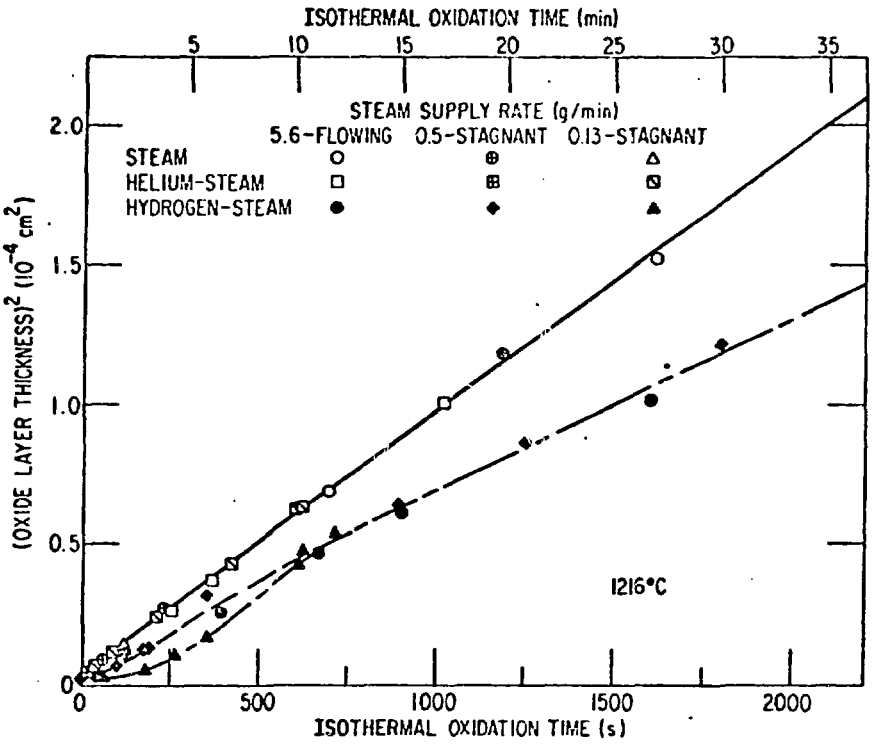

Fig. 4. Square of Oxide Layer Thickness vs Isothermal Oxidation Time Obtained from Zircaloy-4 Oxidation Tests at 1216°C in Pure Steam and Helium-Steam and Hydrogen-Steam Mixtures under Various Steam Flow Conditions. Helium and hydrogen overpressures were essentially identical, i.e., ~33 kPa at 20°C. Total pressures during tests were 38-43 kPa.

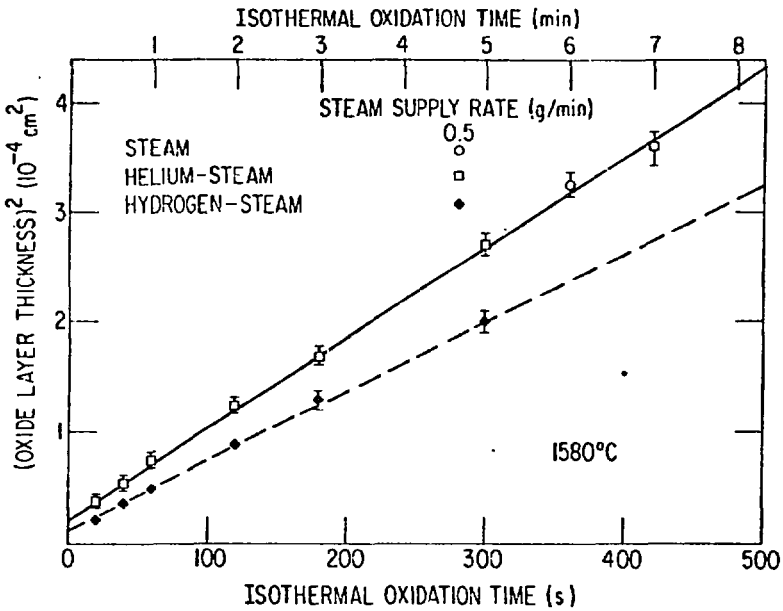

Fig. 5. Square of Oxide Layer Thickness vs Isothermal Oxidation Time Obtained from Zircaloy-4 Oxidation Tests at 1580°C in Pure Steam and Helium-Steam and Hydrogen-Steam Mixtures under Various Steam Flow Conditions. Helium and hydrogen overpressures were essentially identical, i.e., ~33 kPa at 20°C. Total pressures during tests were 38-45 kPa.

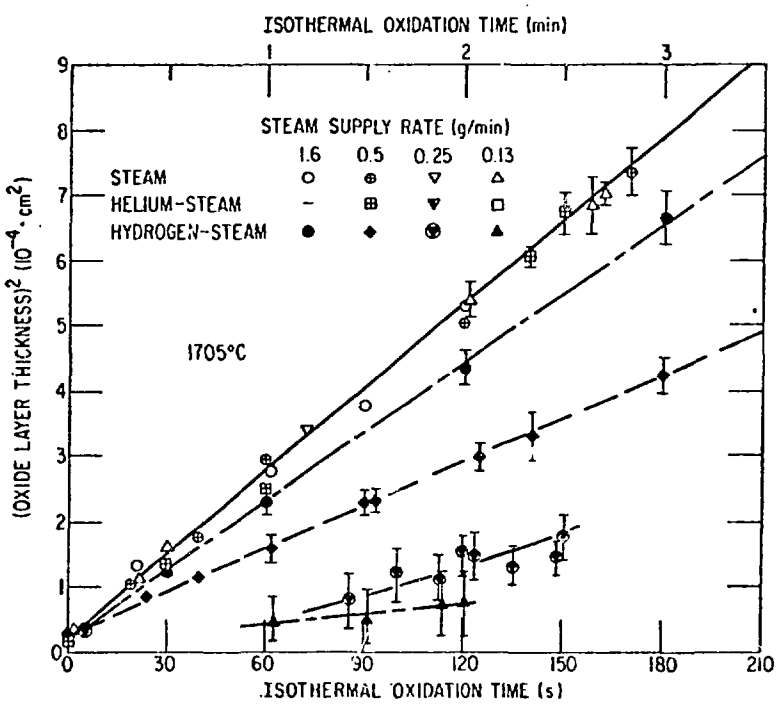

Fig. 6. Square of Oxide Layer Thickness vs Isothermal Oxidation Time Obtained from Zircaloy-4 Oxidation Tests at 1705°C in Pure Steam and Helium-Steam and Hydrogen-Steam Mixtures under Various Steam Flow Conditions. Helium and hydrogen overpressures were essentially identical, i.e., ~33 kPa at 20°C. Total pressures during tests were 38-45 kPa.

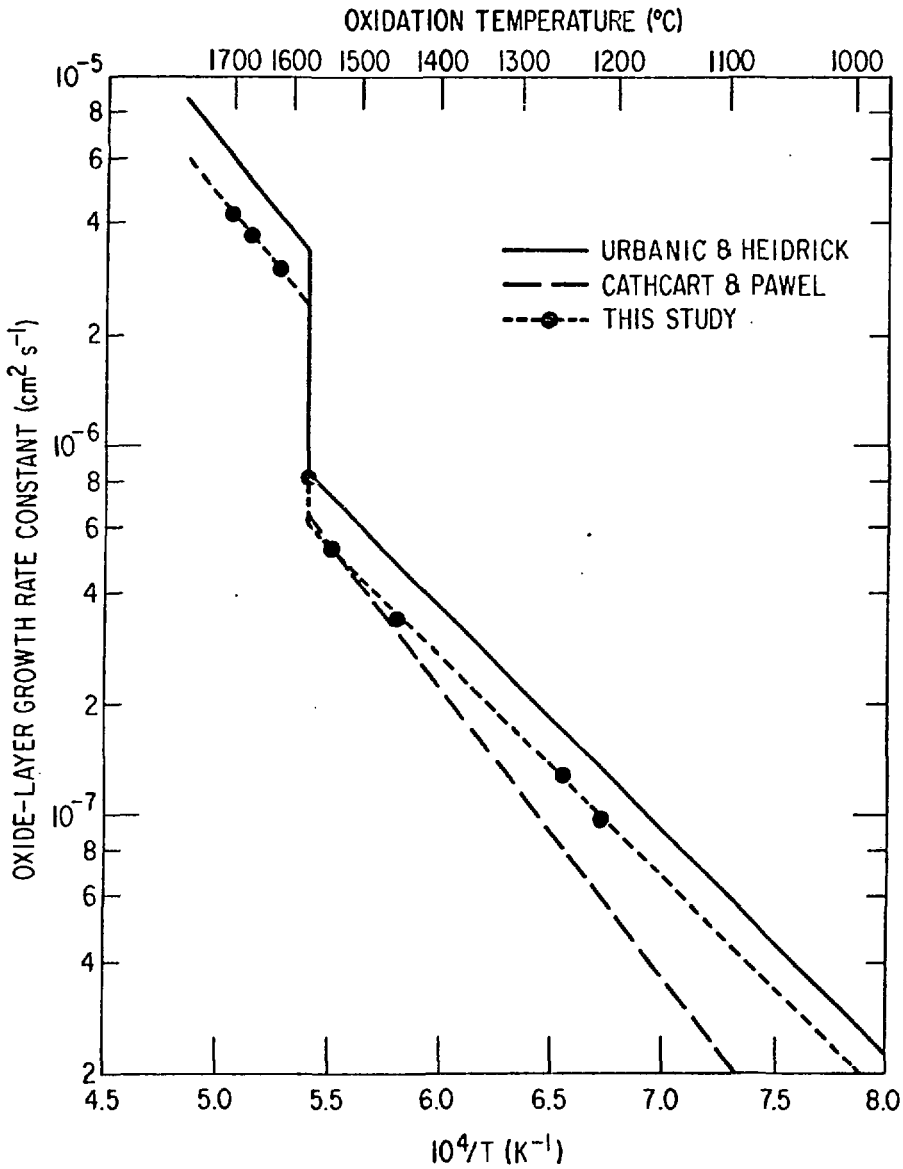

Fig. 7. Parabolic Oxide Layer Growth Rate Constants Obtained for Pure Steam Environments vs Inverse Temperature. Similar results reported by Cathcart and Pawel[4] and Urbanic and Heidrick[7] are shown also for comparison.

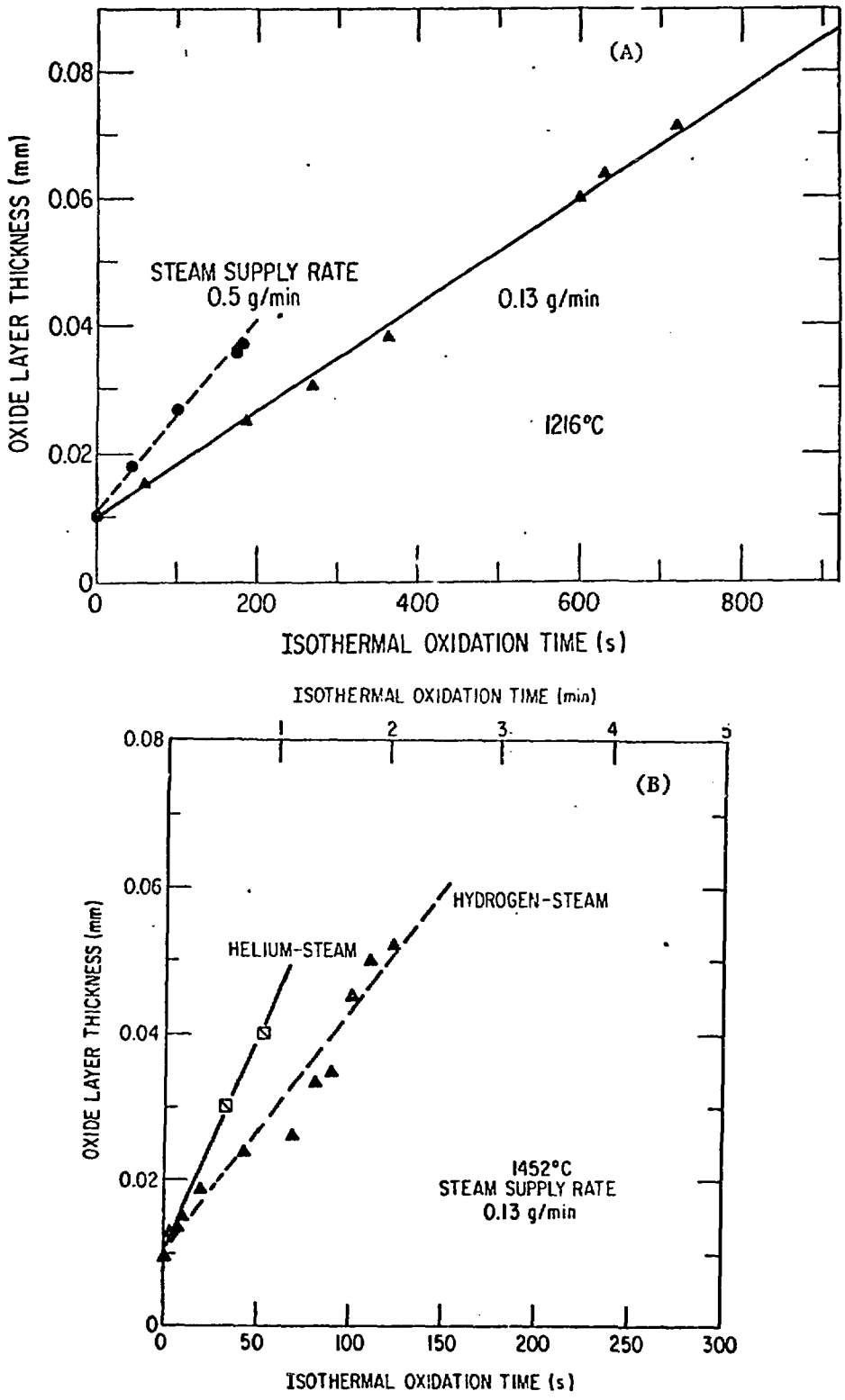

Fig. 8. Oxide Layer Thickness vs Isothermal Oxidation Time for Early Stages of Zircaloy-4 Oxidation in Hydrogen-Steam Mixtures That Show Linear Oxidation Kinetics. (A) Oxidation at 1216°C for steam supply rates of 0.5 and 0.13 g/min, (B) oxidation at 1452°C for a steam supply rate of 0.13 g/min in helium-steam and hydrogen-steam. Stagnant hydrogen or helium overpressure was ~36 kPa at test

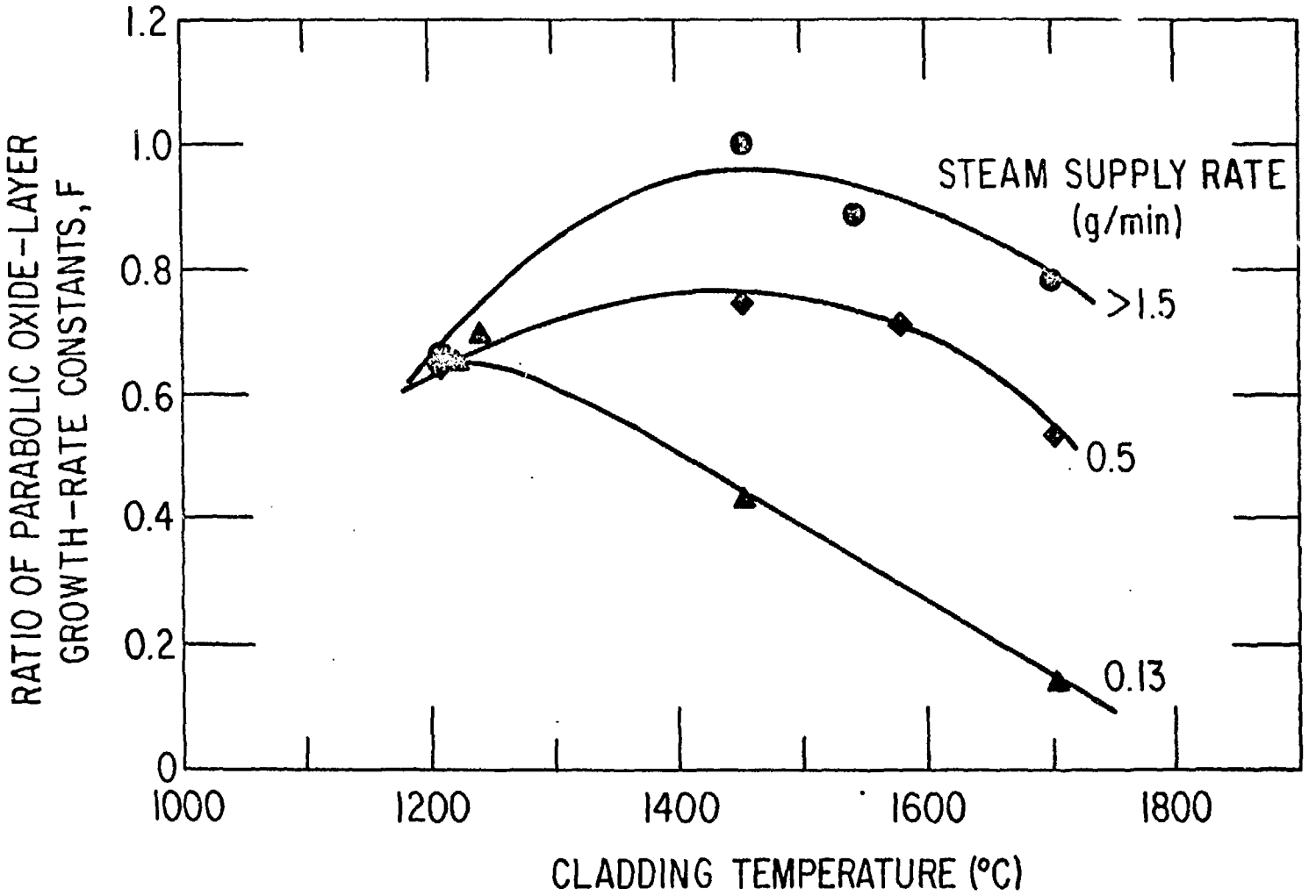

Fig. 9. Ratios (F) of Parabolic Oxide Layer Growth Rate Constant in Hydrogen-Steam Mixtures to That in Unlimited Pure Steam as a Function of Zircaloy-4 Cladding Temperature. The hydrogen overpressure was ~36 kPa and the steam supply rate was varied as indicated.